Pergamon

Int. J. Heat Mass Transfer. Vol. 40, No. 11, pp. 2539–2547, 1997

Printed in Great Britain
0017-9310/97 \$17.00+0.00

PII: S0017-9310(96)00307-9

Oxygen-enhanced/natural gas flame radiation

CHARLES E. BAUKAL and BENJAMIN GEBHART

Mechanical Engineering and Applied Mechanics, University of Pennsylvania, Philadelphia, PA 19104-6315, U.S.A.

(*Received* 12 *July* 1996 *and in final form* 26 *August* 1996)

Abstract—Total radiation measurements for oxygen-enhanced/natural gas diffusion flames are reported here. The parameters that were studied included the oxidizer composition ($\Omega = 0.25$–1.00), the burner firing rate ($q_f = 3$–28 kW), the equivalence ratio ($\phi = 0.55$–1.45), and the axial ($L_r = 0.5$–6.5) and radial ($D_r = 0.4$–1.0) position of the radiometer. The measured radiation ranged from 10 to 65 kW m^{-2}. The nozzle Reynolds numbers ranged from 480 to 10 300. The location of the peak flame radiation ranged from 9 to 15% of the visible flame length. The stability limits and visible flame heights are also reported for a burner with a wide operating range. © 1997 Elsevier Science Ltd. All rights reserved.

INTRODUCTION

For direct flame impingement heating, six modes of heat transfer have been identified in previous studies [1]. These modes include conduction (steady-state and transient), convection (forced and natural), thermochemical heat release (equilibrium, catalytic and mixed), radiation (nonluminous, luminous, and surface), condensation, and boiling (internal and external). Viskanta notes that fundamental knowledge is lacking for the relative importance of radiation vs forced convection in flame impingement heat transfer [2]. That issue is considered here.

Oxygen-enhanced flames use an oxidizer that has a higher concentration of O_2 than is normally found in air ($\Omega = 0.21$). This is the first study of radiative heat flux from oxygen-enhanced natural gas jet flames. The objectives of this work were: (1) to design a burner capable of using an oxidizer ranging from air to pure O_2 ($\Omega = 0.21$–1.00); (2) to determine if nonluminous flame radiation is important in flame impingement heating; (3) to determine how nonluminous flame radiation is influenced by the oxidizer composition, the fuel flow rate, and the equivalence ratio; and (4) to determine how the radiation measurements are influenced by the radiometer location.

NONLUMINOUS FLAME RADIATION

Tien and Lee [3] have reviewed flame radiation. Viskanta and Mengüç [4] reviewed radiation in combustion systems, including flame radiation. Both of these reviews primarily considered radiation modeling from both nonluminous and luminous flames. Other related reviews have been given [5–7]. These have emphasized luminous radiation which is important in fires. The effects of oxygen-enhanced combustion were not considered in any of the above reviews.

The combustion of hydrocarbon fuels produces, among other things, CO_2 and H_2O. These gaseous products generate nonluminous or gaseous radiation which has been extensively studied (e.g. [8]). This heat transfer mode depends on the gas temperature, the partial pressure and concentration of each species, and the molecular path length through the gas [9]. It is also wavelength dependent. This type of radiation is the primary subject of the research presented here.

Table 1 shows the flame impingement studies that have considered nonluminous radiation. More detailed information about the experimental conditions [10] and about the experimental methods and data [11] are given elsewhere. Kilham and co-workers used a thermopile normal to the surface of heated refractory cylinders [12, 13]. The measured radiation was the sum of the radiation from the combustion products flowing around the cylinder and from the cylinder surface. Two screens with narrow slit openings were placed between the flame and the detector to limit the field of view to a small region around the heated cylinder. Kilham [12] found that the nonluminous radiation to the cylinder ranged from 5 to 16% of the total heat flux. However, Jackson and Kilham [13] determined that nonluminous radiation never exceeded 5% of the total heat flux. Since the total flux ranged from 20 to 107 kW m^{-2}, the nonluminous radiation would not have exceeded 5.4 kW m^{-2}. Dunham [14] measured total heat fluxes from 41 to 95 kW m^{-2}. The nonluminous radiation was calculated to be up to 13% of the total flux. Therefore, it would not have exceeded 12 kW m^{-2}.

Shorin and Pechurkin [15] used a steady-state cooled gage to measure the total heat flux from impinging flames. The gage was imbedded flush with the surface of a large plane surface. To determine the importance of radiation, gages with polished, oxidized and blackened surfaces were tested. The lowest flux was expected to be measured for the polished gage

NOMENCLATURE

d	diameter
D	dimensionless diameter $= d/d_n$
l	length
L	dimensionless length $= l/d_n$
q''_{rad}	radiant heat flux
q_f	burner firing rate (kW)
Re	Reynolds number.

Greek symbols

Ω	oxygen enrichment ratio = oxygen volume in the oxidizer/total oxidizer volume
ϕ	equivalence ratio = (stoichiometric oxygen/fuel volume ratio)/(actual oxygen/fuel volume ratio)
θ	view angle.

Subscripts

f	flame
max rad	axial location of peak flame radiation
n	nozzle
r	radiometer.

which reflects most of the radiation. Higher fluxes were expected with the oxidized and blackened gages which are better absorbers. However, no difference in the measured heat flux was found. It was concluded that radiation was not important for those experimental conditions.

Purvis [16] found that the calculated nonluminous flame radiation was negligible compared to the total heat flux which ranged from 950 to 1500 kW m^{-2}. Hoogendoorn *et al.* [17] measured total heat fluxes ranging from 0 to 560 kW m^{-2}. Flame radiation was said to be, at most, 5% of the total heat flux. Therefore, it would not have exceeded 28 kW m^{-2}. No radiation measurements or calculations were given. Davies [18] measured total heat fluxes ranging from 330 to 3400 kW m^{-2}. Using an estimated flame emissivity of 0.01, the calculated nonluminous radiation was said to be only 2% of the total flux. Therefore, it would not have exceeded 68 kW m^{-2}. Ivernel and Vernotte [19] calculated the radiation from oxygen-enhanced natural gas flames. The flame emissivity was estimated using the measured temperature and gas concentrations along with the Hottel charts [8]. The calculated flame radiation was from 7 to 34% of the total measured heat flux to the hemi-nosed cylinder. Van der Meer [20] stated that the flame radiation in his study was negligible because of the very low emissivity of a thin hot gas layer. No supporting calculations were cited.

In most of the previous studies, nonluminous flame radiation was found to be negligible compared to the total heat flux from an impinging flame. Only the studies by Davies [18] and Ivernel and Vernotte [19] considered oxidizers other than air or pure O_2. The nonluminous flame radiation was not measured in either study. The maximum reported radiant flux of 90 kW m^{-2} was for a pure O_2 oxidizer.

OXYGEN-ENHANCED FLAMES

For industrial burners, a fossil fuel is typically combusted with air. Air contains approximately 21% O_2 and 79% N_2 by volume. However, only the O_2 in the air actively participates in the chemical reactions. The N_2 is mostly a diluent which can also lead to harmful NO_x pollutant emissions. The combustion process may be enhanced by using oxidizers with higher concentrations of O_2. One result is an increase in the adiabatic flame temperature as shown in Fig. 1. Higher flame temperatures lead to higher productivity in heating processes. Other common benefits of using oxygen-enhanced flames include higher thermal efficiencies, higher burner turndown ratios, improved flame stability, lower exhaust gas volumes, and lower pollutant emissions [21].

For hydrocarbon flames, nonluminous radiation comes exclusively from carbon dioxide and water vapor [3]. Another important result of enhancing flames with oxygen is the change in the concentrations of CO_2 and H_2O, as Ω increases. The predicted volume concentrations of CO_2 and H_2O are shown in Fig. 2. This plot is for the adiabatic equilibrium, stoichiometric combustion of the natural gas used in this

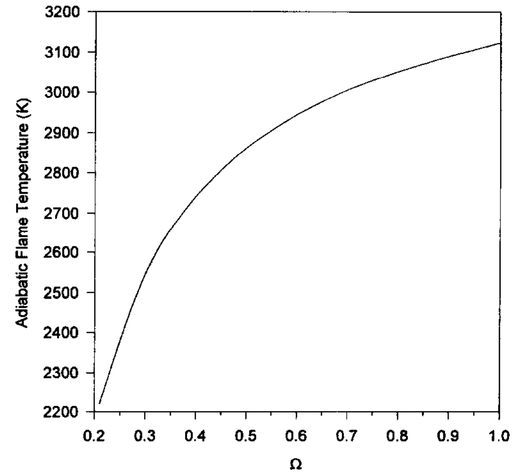

Fig. 1. Predicted flame temperature vs oxidizer composition (N_2+O_2), for the adiabatic equilibrium combustion of the natural gas used in this study.

Table 1. Summary of previous flame impingement studies considering nonluminous radiation

Fuel	Ω	ϕ	Flow geometry	q''_{rad} (kW m^{-2})	Reference
CO	0.21	1.0, 1.19	laminar axisymmetric flame normal to uncooled refractory cylinder	4.0–17.1	Kilham (1949)
H_2	0.21	1.0	laminar axisymmetric flame normal to uncooled refractory cylinder	negligible	Jackson and Kilham (1956)
H_2	1.00	1.0		(>5.4)	
CO	1.00	1.0, 2.0			
CO	0.21	0.7–1.3	laminar axisymmetric flame normal to cooled hemi-nosed brass cylinder	up to 12	Dunham (1963)
Town gas	0.21	0.67–0.95	laminar and turbulent axisymmetric flames normal to cooled flat metal plate	negligible	Shorin & Pechurkin (1968)
CH_4	1.00	0.95–1.31	laminar axisymmetric flame normal to uncooled flat refractory plate	negligible	Purvis (1974)
C_3H_8	1.00	1.45–1.83			
Natural gas	0.21	1.0	laminar axisymmetric flame normal to a cooled flat copper plate	negligible (<28)	Hoogendoorn *et al.* (1978)
Natural gas	0.21	0.6–1.3	slot-shaped flame normal to water-cooled stainless steel cylinder	negligible	Davies (1979)
	0.29–0.53	0.5–1.3		(<68)	
	1.00	0.5–1.16			
Natural gas	0.25	0.95	turbulent axisymmetric flame normal to uncooled hemi-nosed inconel cylinder	20–25	Ivernel & Vernotte (1979)
	0.50	0.95		45–65	
	1.00	0.95		50–90	
Natural gas	0.21	1.0	laminar and turbulent axisymmetric flames normal to cooled flat copper plate	negligible	van der Meer (1987)
Natural gas	0.21	1.00	laminar and turbulent flames	10	This study
	0.28–0.9	0.55–1.45		15–63	
	1.00	0.55–1.45		20–65	

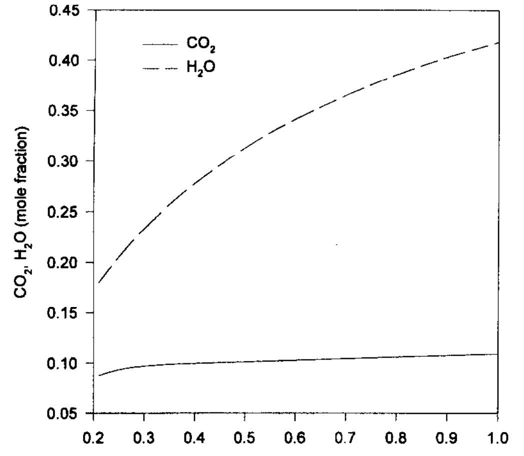

Fig. 2. Predicted CO_2 and H_2O mole fractions vs oxidizer composition (N_2+O_2), for the adiabatic equilibrium combustion of natural gas.

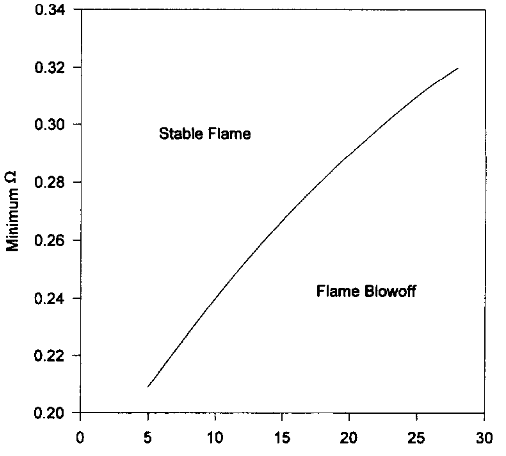

Fig. 3. Burner operating regime.

study. Higher gas temperatures and concentrations of CO_2 and H_2O are both important in nonluminous flame radiation. Nonluminous radiation measurements do not appear to have been made for oxygen-enhanced free jet flames. Viskanta [22] feels that knowledge of radiation in those flames is lacking. The results presented here consider that issue.

EXPERIMENTAL APPARATUS

Burner

One task of this research was to design a burner that could operate on natural gas with oxidizers ranging from air to pure O_2. A number of burners were fabricated generally consisting of concentric rings of evenly distributed small diameter fuel tubes [23]. A variety of oxidizer hole patterns were tested ranging from a series of concentric holes drilled through a thin plate, to a completely open oxidizer passage (no plate). Both diffusion and premixed configurations were tested. In addition, several burners were purchased and tested, along with modifications.

The burner that had the widest operating range was a modified version of a model number ICSM 35 manufactured by Nordsea Gas Technology Ltd (Cheshire, England). The water-cooled burner body was made of hastalloy. The effective nozzle diameter, d_n, was 38.5 mm. The matrix of mixture outlet pairs consisted of three concentric rows surrounding one central pair. Each mixture outlet pair consisted of a square tube located inside a round tube, which created two passages. The fuel gas flowed through the inner passage which was the internal cross-sectional area of the square tube. The oxidizer flowed through the outer passage which was the area between the internal diameter of the round tube and the outer cross-sectional area of the square tube. Details of the burner geometry are given elsewhere [23]. The burner was fired vertically upward into a large exhaust hood.

The original burner was primarily designed to operate with a pure O_2 oxidizer. The burner was modified by adding additional oxidizer ports. These were required because of the added volume as more N_2 was included in the oxidizer. The original burner had a slightly fuel rich zone in the center of the burner. To make the flame more uniform, the oxidizer holes in the center of the burner were larger than the outer sets of holes. One of the key aspects of the burner design was the uniform, nearly one-dimensional flame that it produced.

The natural gas used for this study had the following typical composition by volume: 95.278% CH_4, 2.539% C_2H_6, 0.544% C_3H_8, 0.197% C_4H_{10}, 0.068% C_5H_{12}, 0.028% C_6H_{14}, 0.020% C_7H_{16}, 0.005% C_8H_{18}, 0.869% CO_2, 0.417% N_2, 0.023% H_2, 0.008% He, 0.002% Ar and 0.002% O_2. The higher heating value was 38.66 MJ m^{-3}. The specific gravity was 0.588. For stoichiometric combustion ($\phi = 1$), 2.044 moles of O_2 were required for each mole of natural gas. The adiabatic flame temperature for this fuel combusted with air and with pure O_2 was 2230 and 3060 K, respectively. The oxidizer was made by blending O_2 (>99.5% purity) with N_2 (>99.998% purity).

The natural gas, O_2, and N_2 flows were measured with Hastings model HFC-203 mass flow meters. The natural gas and O_2 meters had ranges of 0–170 and 0–340 m^3 min^{-1} at STP, respectively. The low and high flow N_2 meters had ranges of 0–170 and 0–1360 m^3 min^{-1} at STP, respectively. The meters were accurate to 1% of their full scale reading.

Figure 3 is a plot of the burner stability limits as a function of the firing rate and oxidizer composition. Above the curve, a stable flame existed. Below the curve, the flame blew off. The highest firing rate shown was a limit of the gas flow control equipment, not of the burner. The lowest firing rate tested was 3 kW. Below that rate, the flame became unsteady due to buoyancy. Figure 4 shows the visible flame length, visually determined in a dark room, as a function of the firing rate for two oxidizer compositions. For low

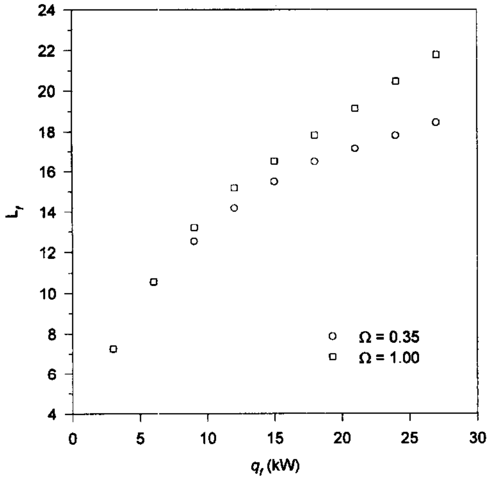

Fig. 4. Visible flame length vs q_f and Ω, ϕ = 1.00.

firing rates, the flame lengths were essentially the same for both oxidizer compositions. At higher firing rates, the flames with higher Ω were longer.

Radiation measurements

An elevation view of the radiometer and flame is shown in Fig. 5(a). A plan view of the arrangement is shown in Fig. 5(b). A Medtherm Corp. model 40-5-18T heat flux transducer was used to measure the radiation. The transducer was a Gardon gage [24] with a diameter of 6.35 mm. The sensor absorptance was 97% in the spectral range of 0.6–15.0 μm. A model 40VRW-7C water-cooled view restrictor was used to restrict the field of view to $\theta_r = 6.45°$. A narrow angle radiometer was used to ensure that only radiation from the flame, not from the ambient environment, would be measured. This is representative of the case for an impinging flame where the target is engulfed by the hot combustion gases. The radiometer did not have any windows or gas purging since the environment was clean. The water-cooled sensor body temperature was measured with a type T thermocouple and was approximately a constant 292 K. The certified calibration of the gage, with the view restrictor, was accurate to 3%. The heat flux range of this gage was 0–57 kW m^{-2}. The response was linear up to 150% of that range. At low firing rates, the measured radiation fluctuated the most due to the buoyancy of the flames. For those flames, the highest uncertainty was estimated to be 9.3%. The typical uncertainty was less than 5%.

The vertical burner position was controlled with an electric actuator with a potentiometer output to indicate the position. The distance between the burner and the radiometer was manually adjusted with a

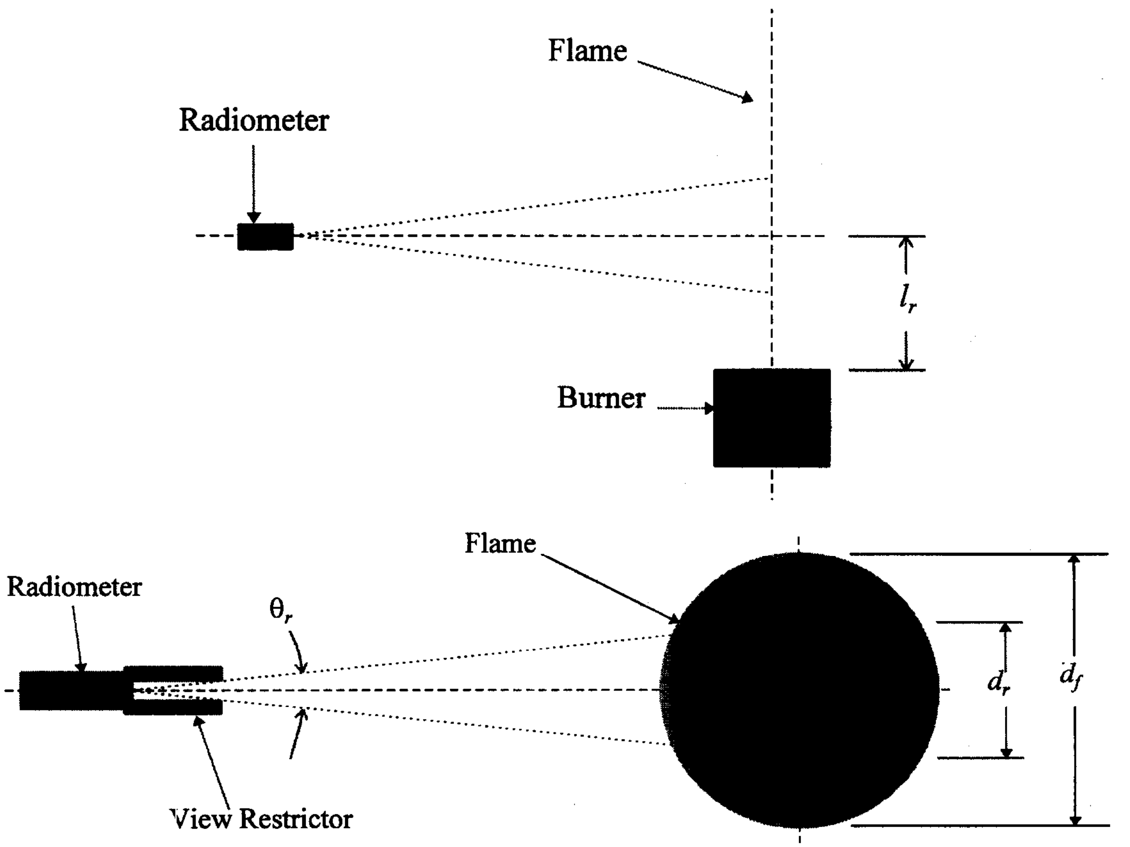

Fig. 5. (a) Elevation view of radiometer and flame; (b) plan view of radiometer and flame.

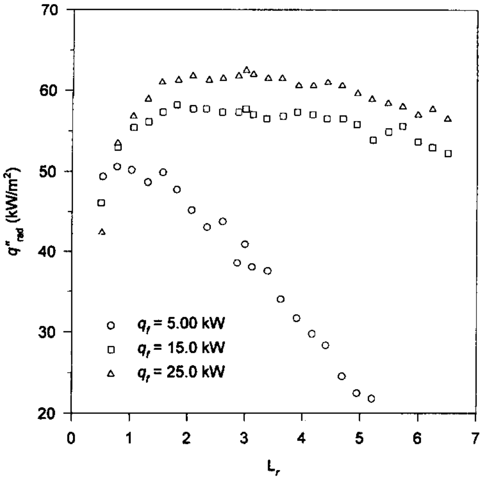

Fig. 6. q''_{rad} vs L_r and q_f (5.0, 15.0, 25.0 kW) for $\Omega = 1.00$, $\phi = 1.00$, $D_r = 0.5$.

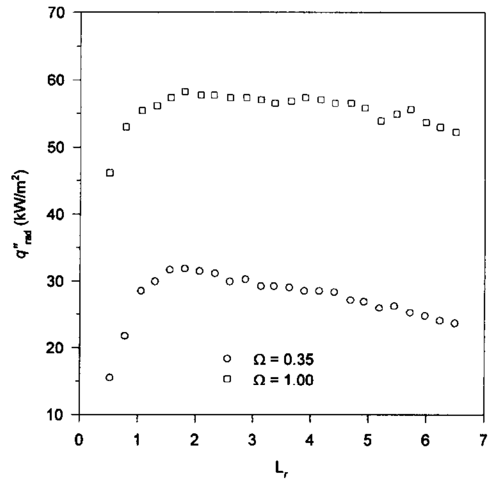

Fig. 7. q''_{rad} vs L_r and Ω (0.35, 1.00) for $q_f = 15.0$ kW, $\phi = 1.00$, $D_r = 0.5$.

machinists's milling table. The positions were accurate to within 0.5 mm.

RESULTS AND DISCUSSION

Five parameters were investigated including the burner firing rate (q_f), the oxidizer composition (Ω), the equivalence ratio (ϕ), the axial position along the flame (L_r), and the radial position from the flame (D_r). The parameters of primary interest were Ω, q_f, and L_r. Most of the tests were done at $\phi = 1.0$ and $D_r = 0.5$. The equivalence ratio was only varied through a narrow range for two reasons. The first is that the equivalence ratio is operated in a narrow band around stoichiometric conditions in nearly all industrial heating and melting processes. The second reason is that only nonluminous radiation was studied here. If the burner were operated at very fuel rich conditions ($\phi \to \infty$), luminous radiation would have become important.

Radiometer position

The first set of tests was designed to determine how the axial and radial position of the radiometer affected the flame radiation measurements.

Axial location. Figure 6 shows the effects of both the firing rate and the axial distance along the flame length. The minimum L_r was 0.5. For $L_r < 0.5$, the radiometer would have viewed the flame and part of the burner itself. At low firing rates, the flame radiation decreased rapidly with the distance from the burner exit. At the intermediate and higher firing rates, the flame radiation was relatively constant for L_r from about 2–5. Therefore, $L_r = 3.0$ and $q_f = 15.0$ kW were used as fixed parameters in some of the subsequent tests because of the constancy of the radiant flux. Figure 7 is a similar graph except that the oxidizer composition, instead of the firing rate, was varied. The flame radiation was relatively constant over a wide range of L_r, for $\Omega = 1.0$. At $\Omega = 0.35$, the peak flame radiation occurred at about $L_r = 1.5$ and then slowly decreased with L_r.

Radial position. Figure 8 shows how the radial location of the radiometer affected the measurements. At $D_r = 1.0$, the radiometer viewed the entire width of the flame. The effective path length decreased as D_r increased because the flame had a circular cross section. This reduced the average flame radiation as shown in the plot. However, the reduction was relatively small. Therefore, subsequent tests were done at $D_r = 0.5$.

Burner operating conditions

The burner operating conditions include the equivalence ratio, the oxidizer composition, and the firing rate.

Equivalence ratio. Figure 9 shows how the equivalence ratio and the oxidizer compositions affected the flame radiation. For the smaller Ω, the highest flame radiation occurred at slightly fuel lean

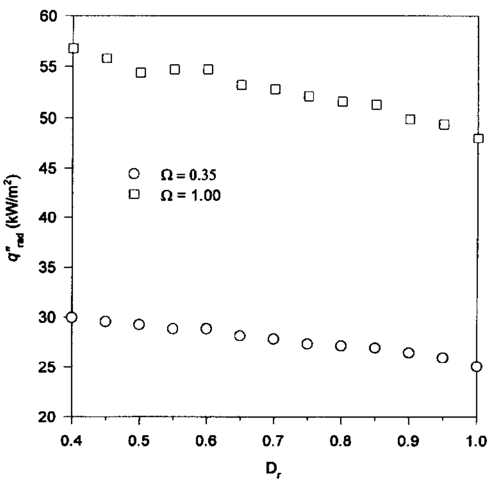

Fig. 8. q''_{rad} vs D_r and Ω (0.35, 1.00) for $q_f = 15.0$ kW, $\phi = 1.00$, $L_r = 3.0$.

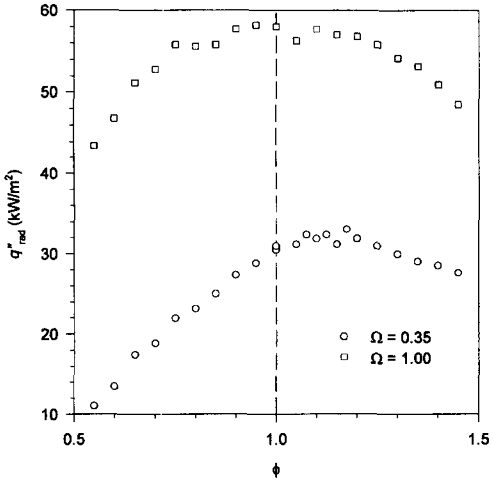

Fig. 9. q''_{rad} vs ϕ and Ω (0.35, 1.00) for q_f = 15.0 kW, L_r = 3.0, D_r = 0.5.

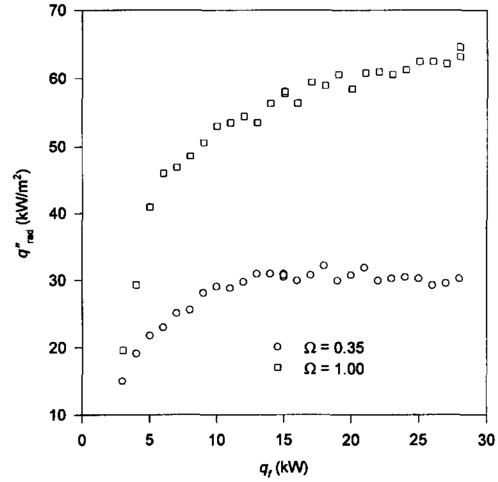

Fig. 11. q''_{rad} vs q_f and Ω (0.35, 1.00) for ϕ = 1.00, L_r = 3.0 and D_r = 0.5.

conditions. For a pure O_2 oxidizer, the highest flame radiation occurred in a band around stoichiometric conditions (ϕ = 1.0).

Oxidizer composition. Figure 10 shows how the flame radiation varied as a function of the oxidizer composition, for a fixed firing rate and equivalence ratio. The only thing that was varied was the amount of N_2 in the oxidizer. The fuel and O_2 flow rates were constant. Re_n decreased from 6800 to 2400 as Ω increased from 0.28 to 1.00. The plot shows that the flame radiation increased by more than 2.5 times by removing N_2 from the oxidizer. As previously discussed, this is a result of higher flame temperatures and partial pressures of CO_2 and H_2O.

Most of the measurements in Table 1 were made with air as the oxidizer. A similar measurement was made in the present study at Ω = 0.21. As shown in Fig. 3, the highest firing rate for a stable air/natural gas flame was 5 kW. This rate was used since the radiation measurements were less uncertain at higher firing rates. For a stoichiometric flame (ϕ = 1.00) at D_r = 0.5, the peak measured flame radiation was 9.5 kW m^{-2} at $L_r \approx 1.3$.

Firing rate. Figure 11 shows how the flame radiation increased as the firing rate increased and as the equivalence ratio increased. Figure 12 is a plot of flame radiation as a function of the equivalence ratio and the firing rate for a constant Reynolds number of 4500. As N_2 was removed from the oxidizer (Ω increasing), the firing rate had to be increased to maintain a fixed Re_n. This shows that a higher heat release density may be achieved by increasing the O_2 concentration in the oxidizer, for a given nozzle diameter. It also implies that Re_n by itself is not a sufficient parameter to indicate the performance of oxygen-enhanced flames. The oxidizer composition Ω must also be specified.

Figure 13 shows the peak flame radiation measured for a given firing rate and oxidizer composition. For Ω = 1.00, the peak radiation increased with the firing rate. For Ω = 0.35, the peak radiation was relatively

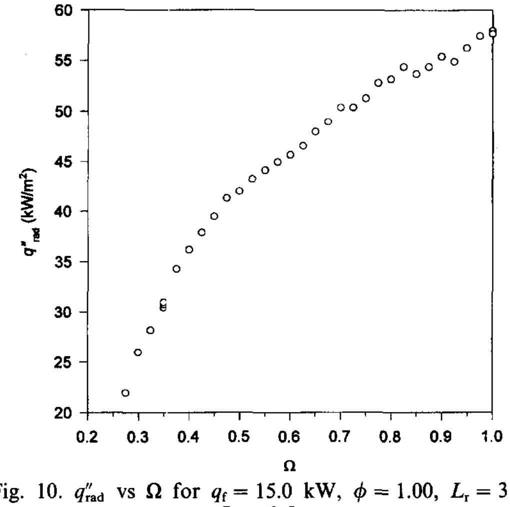

Fig. 10. q''_{rad} vs Ω for q_f = 15.0 kW, ϕ = 1.00, L_r = 3.0, D_r = 0.5.

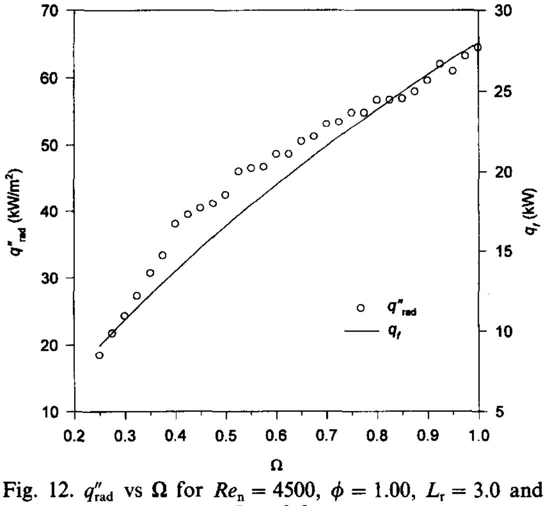

Fig. 12. q''_{rad} vs Ω for Re_n = 4500, ϕ = 1.00, L_r = 3.0 and D_r = 0.5.

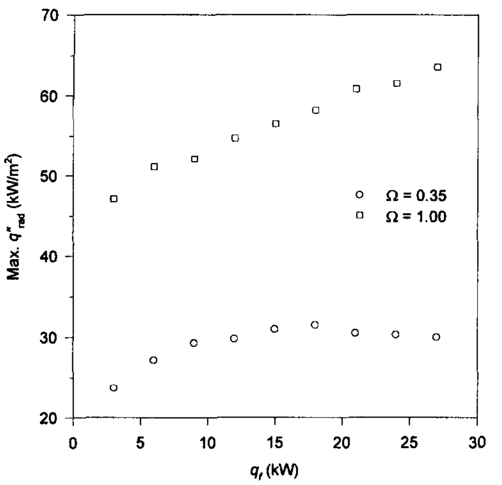

Fig. 13. Maximum q''_{rad} vs q_f and Ω (0.35, 1.00) for $\phi = 1.00$ and $D_r = 0.5$ with L_r variable.

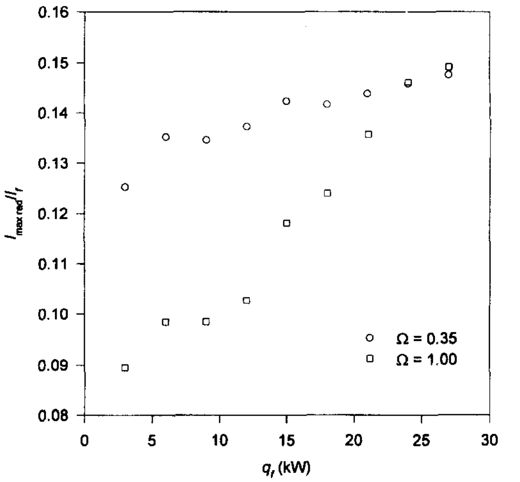

Fig. 15. $l_{max\,rad}/l_f$ vs q_f and Ω (0.35, 1.00) for $\phi = 1.00$ and $D_r = 0.5$.

constant over a wide range of firing rates. Figure 14 shows the approximate axial location for the peak flame radiation. Initially, the peak flame locations were closer to the burner for $\Omega = 1.00$, compared to $\Omega = 0.35$. At higher firing rates, this trend reversed. For $\Omega = 1.00$, these locations were fairly well defined. For $\Omega = 0.35$, there was a range of positions along the flame length where the maximum flame radiation values were obtained. The locations given in the figure are approximately in the center of the range. Figure 15 is a plot of the location for the peak flame radiation which has been normalized to the length of the flame (see Fig. 4). This shows that for high Ω flames, the axial location of the peak flame radiation was at about 14% of the visible flame length. For the lower Ω flames, this location was between about 9 and 15% of the flame length.

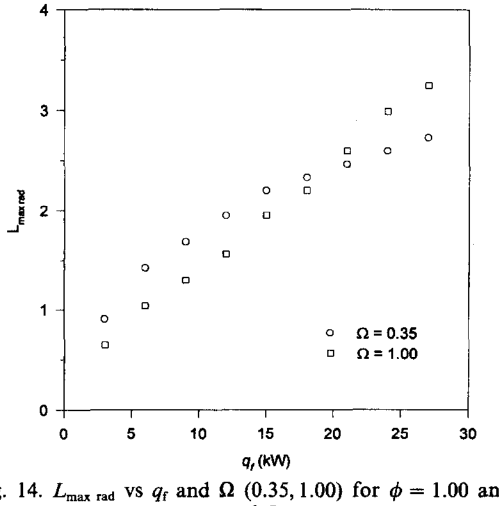

Fig. 14. $L_{max\ rad}$ vs q_f and Ω (0.35, 1.00) for $\phi = 1.00$ and $D_r = 0.5$.

CONCLUSIONS

A new burner design was reported which produced a uniform flame with oxidizers ranging from air to pure O_2. This is the first paper to report nonluminous flame radiation as a function of the oxidizer composition. It has been shown that the thermal radiation increased dramatically by removing N_2 from the oxidizer. The flame radiation increased with the firing rate. The increase was more dramatic at higher O_2 concentrations in the oxidizer. Higher flame radiation was measured at or near stoichiometric conditions where typical industrial heating processes are operated. For higher firing rates, the radiation was nearly constant over a wide range of axial locations in the flame. At lower firing rates, the flame radiation decreased with the axial distance from the burner outlet.

For higher O_2 concentrations, the peak flame radiation increased with the firing rate. For lower O_2 concentrations, the peak flame radiation was nearly constant over a wide range of firing rates. The location of the peak flame radiation varied from 9 to 15% of the visible flame length. This location was more defined for the higher O_2 flames in terms of both its absolute position and of the position normalized by the flame length.

The radiant fluxes reported here are comparable to the data from previous studies. However, these measured radiant fluxes are not significant (< 10%) compared to the total heat fluxes reported for flames impinging on a target [23]. Therefore, nonluminous flame radiation does not appear to be an important mechanism in flame impingement heating. This may be an advantage in some industrial heating applications. The heat flux to low emissivity targets, such as finished metal sheets or slab, will not be adversely affected by reduced radiant absorption.

Acknowledgements—Funding for this research was provided by Air Products and Chemicals, Inc. (Allentown, PA) and by Gas Research Institute (Chicago, IL) under the project entitled "Development of a Rapid Heater for Metal Reheating" (GRI contract no. 5088-235-1683).

REFERENCES

1. Baukal, C. E., Farmer, L. K., Gebhart, B. and Chan, I., Heat transfer mechanisms in flame impingement heating. *Proceedings of the* 1995 *International Gas Research Conference*, ed. D. A. Dolenc, Vol. 2. Government Institutes, Inc., Rockville, MD, 1996, pp. 2277-2287.
2. Viskanta, R., Heat transfer to impinging isothermal gas and flame jets. *Experimental Thermal Fluid Science*, 1993, **6**, 111-134.
3. Tien, C. L. and Lee, S. C., Flame Radiation, *Progress in Energy Combustion Science*, 1982, **8**, 41-59.
4. Viskanta, R. and Mengüç, M. P., Radiation heat transfer in combustion systems. *Progress in Energy Combustion Science*, 1987, **13**, 97-160.
5. De Ris, J., Fire radiation—a review. *17th Symposium (International) on Combustion*. The Combustion Institute, Pittsburgh, PA, 1978, pp. 1003-1016.
6. Faeth, G. M., Heat transfer is fires and combustion systems. *Proceedings of the* 1988 *National Heat Transfer Conference*, ed. H. R. Jacobs, HTD-Vol. 96, Vol. 1. ASME, New York, 1988, pp. 1-25.
7. Faeth, G. M., Gore, J. P., Chuech, S. G. and Jeng, S. M., Radiation from turbulent diffusion flames. *Annual Review of Numerical Fluid Mechanics and Heat Transfer*, 1988, **2**, 1-38.
8. Hottel, H. C. and Sarofim, A. F., *Radiative Transfer*. McGraw-Hill, New York, 1967, Chap. 6.
9. Siegel, R. and Howell, J. R., *Thermal Radiation Heat Transfer*, 3rd edn. Hemisphere, Washington, D.C. 1992, chap. 13.
10. Baukal, C. E. and Gebhart, B., A review of flame impingement heat transfer—Part 1: experimental conditions. *Combustion Science Technology*, 1995, **104**(4-6), 339-357.
11. Baukal, C. E. and Gebhart, B., A review of flame impingement heat transfer—Part 2: measurements. *Combustion Science Technology*, 1995, **104**(4-6), 359-385.
12. Kilham, J. K., Energy transfer from flame gases to solids. *3rd Symposium on Combustion and Flame and Explosion Phenomena*. The Williams and Wilkins Co., Baltimore, MD, 1949, pp. 733-740.
13. Jackson, E. G. and Kilham, J. K., Heat transfer from combustion products by forced convection. *Industrial Engineering Chemistry*, 1956, **48**(11), 2077-2079.
14. Dunham, P. G., Convective heat transfer from carbon monoxide flames. Ph.D. thesis, The University of Leeds, Leeds, U.K., 1963.
15. Shorin, S. N. and Pechurkin, V. A., Effectivnost' teploperenosa na poverkhnost' plity ot vysokotemperaturnoi strui produktov sjoraniya razlichnykh gazov. *Teoriya i Praktika Szhiganiya Gaza*, 1968, **4**, 134-143.
16. Purvis, M. R. I., Heat transfer from normally impinging hydrocarbon oxygen flames to surfaces at elevated temperatures. Ph.D. thesis, The University of Leeds, Leeds, U.K., 1974.
17. Hoogendoorn, C. J., Popiel, C. O. and van der Meer, T. H., Turbulent heat transfer on a plane surface in impingement round premixed flame jets. *Proceedings of 6th International Heat Transfer Conference*, 1978, **4**, 107-112.
18. Davies, D. R., Heat transfer from working flame burners. B.S. thesis, University of Salford, Salford, U.K., 1979.
19. Ivernel, A. and Vernotte, P., Etude expérimentale de l'amélioration des transferts convectis dans les fours par suroxygénation du comburant. *Revue Gén. Therm., Fr.*, 1979 (210-211), 375-391.
20. van der Meer, T. H., Heat transfer from impinging flame jets, Ph.D. thesis, Techincal University of Delft, the Netherlands, 1987.
21. Baukal, C. E., Eleazer, P. B. and Farmer, L. K., Basis for enhancing combustion by oxygen enrichment. *Industrial Heating*, 1992, 22-24.
22. Viskanta, R., Enhancement of heat transfer in industrial combustion systems: problems and future challenges, *Proceedings of the ASME/JSME Thermal Engineering Joint Conference*, Vol. 5. ASME, New York, 1991, pp. 161-173.
23. Baukal, C. E., Heat transfer from flames impinging normal to a plane surface, Ph.D. thesis, University of Pennsylvania, Philadelphia, Pennsylvania, 1996.
24. Gardon, R., A transducer for the measurement of heat flow rate. *Journal of Heat Transfer*, 1960, **82**, 396-398.